ELSEVIER

High-accuracy roundness measurement by a new error separation method

Wei Gao, Satoshi Kiyono and Takamitu Sugawara
Department of Mechatronics, Faculty of Engineering, Tohoku University, Aoba-ku, Sendai, Japan

This paper presents a new error separation method for accurate roundness measurement called the orthogonal mixed method. This method uses the information of one displacement probe and one angle probe to separate roundness error from spindle error. This method was developed from the mixed method, which uses the information of two displacement probes and one angle probe to carry out the error separation. In the present paper, the relationship between the characteristics of the mixed method and the probe arrangement is analyzed. Well-balanced harmonic response of the mixed method is verified to be obtainable for the case where the angular distance between the displacement probe and the angle probe is set at 90°. This orthogonal mixed method also has the simplest probe arrangement, because it requires only one displacement probe and one angle probe to realize the error separation. Optical probes were used to construct an experimental measurement system that employs the orthogonal mixed method. The displacement probe and the angle probe both use the principle of the critical angle method of total reflection, and they have stabilities of 1 nm and 0.01 in., respectively. The measurement results show that roundness measurement can be performed with a repeatability on the order of several nanometers. © 1997 Elsevier Science Inc.

Keywords: metrology; roundness error; spindle error; error separation; optical sensor; displacement probe; angle probe; mixed method; orthogonal mixed method

Introduction

Demand for workpiece roundness measurement to nanometric accuracy is increasing, and on-machine measurement is also required for improving machining accuracy and efficiency. Separation of roundness errors of workpieces from spindle errors of machine tools is essential for accurate measurement of roundness under on-machine conditions.

Error separation techniques[1] employing multiple displacement probes to perform on-machine roundness measurement have been developed. Roundness measurement involves three parameters; roundness error of the workpiece, the *X*-directional component, and *Y*-directional component of the spindle error. The three-point method,[2–9] which employs three displacement probes, can realize the error separation and is in wide use. However, some high-frequency components of roundness error cannot be measured accurately using this method because of the problem of harmonic suppression. Although efforts have been made to overcome this weakness of the three-point method through use of more than three displacement probes,[10–13] the problem of harmonic suppression cannot be completely solved by merely increasing the number of probes.[14]

The authors have proposed a new multiprobe method, named the mixed method.[15] In contrast to

Address reprint requests to Dr. Wei Gao, Department of Mechatronics, Faculty of Engineering, Aramaki Aza Aoba, Aoba-ku, Sendai 980, Japan. E-mail: gaowei@cc.mech.tohoku.ac.jp

Precision Engineering 21:123–133, 1997

655 Avenue of the Americas, New York, NY 10010

0141-6359/97/$17.00
PII S0141-6359(97)00081-0

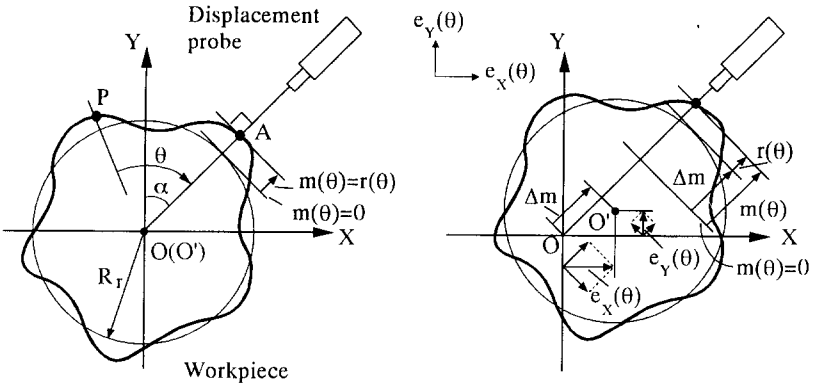

(a) Without spindle error (b) With spindle error

Figure 1 Roundness measurement by a displacement probe: (a) without spindle error; (b) with spindle error

conventional multiprobe methods, this method uses two displacement probes and one angle probe. The mixed method does not suffer the problem of harmonic suppression and can separate roundness error from spindle error with the accuracy of the probes.

In a multiprobe method, matching such characteristics of the probes as frequency responses, linearities and temperature coefficients is very important. For this reason, using the fewest possible probes is desirable, especially when measuring the roundness error to nanometric accuracy.

In the present paper, we investigate the possibility of using fewer probes to realize the mixed method and propose an optimum mixed method called the orthogonal mixed method. This method uses only one displacement probe and one angle probe, arranged at an angular distance of 90° and yields good characteristics. Optical probes were used to construct an experimental measurement system based on the orthogonal mixed method. The effectiveness of the orthogonal mixed method is confirmed by the experimental results.

Roundness measurement using the single-probe method

Figure 1 shows the principle of roundness measurement by one displacement probe.[16,17] A displacement probe, which is fixed spatially, is used to scan a cylindrical workpiece while the workpiece is rotating. Let P be a representative point of the workpiece, the roundness error be described by the function $r(\theta)$, and the local slope of the surface can be described by the function $r'(\theta)$, where θ is the angle between point P and the probe. Let α be the angle between the probe and the Y-axis.

If no rotational error of the spindle exists, as shown in *Figure 1(a)*, the roundness error $r(\theta)$ can be obtained correctly from the probe output $m(\theta)$. However, if spindle error exist, as shown in *Figure 1(b)*, the probe output $m(\theta)$ becomes

$$m(\theta) = r(\theta) + \Delta m(\theta) = r(\theta) + e_X(\theta)\sin\alpha + e_Y(\theta)\cos\alpha \quad (1)$$

where $e_X(\theta)$ and $e_Y(\theta)$ are the X-directional component and the Y-directional component of the spindle error.

As shown in *Figure 2*, we can also use one angle probe to perform roundness measurement. If no spindle error exists, the local slope[18,19] $r'(\theta)$ can be measured correctly by the angle probe, and the roundness error can then be obtained by integrating $r'(\theta)$. However, because of the shift of the measuring point on the circumference of the workpiece, spindle error will generate an angle change $\Delta\mu(\theta)$,[20] causing the probe output to become

$$\mu(\theta) = r'(\theta) + \Delta\mu(\theta) = r'(\theta) + (e_X(\theta)\cos\alpha - e_Y(\theta)\sin\alpha)/R_r \quad (2)$$

where, R_r is the radius of the workpiece.

Error separation using the mixed method

Figure 3 shows the principle of the two displacement-one angle (2D1A) mixed method schematically. Two displacement probes (probes 1 and 3) and one angle probe (probe 2), which are fixed around the workpiece, scan the workpiece simultaneously while it is rotating. Let α and β be the angles between the probes.

If the outputs of the probes are denoted by $m_A(\theta)$, $\mu_B(\theta)$, and $m_C(\theta)$, respectively, then

$$m_A(\theta) = r(\theta) + e_Y(\theta) \quad (3)$$

$$\mu_B(\theta) = r'(\theta + \alpha) + (e_X(\theta) \times \cos\alpha - e_Y(\theta)\sin\alpha)/R_r \quad (4)$$

$$m_C(\theta) = r(\theta + \beta) + e_X(\theta)\sin\beta + e_Y(\theta)\cos\beta \quad (5)$$

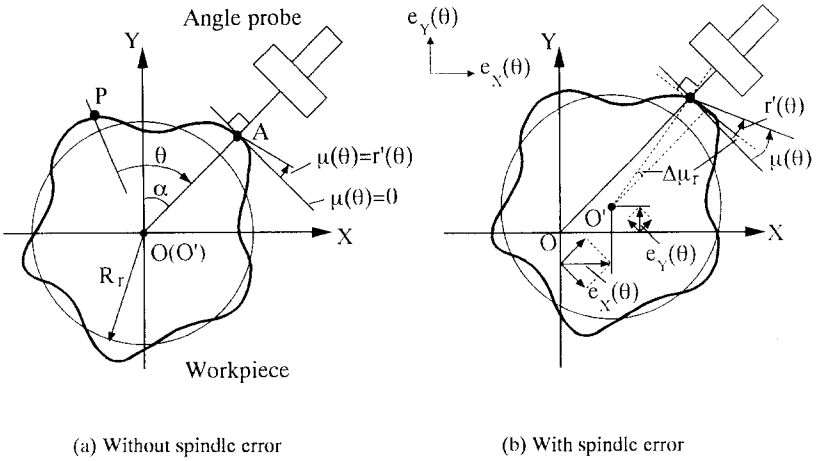

(a) Without spindle error (b) With spindle error

Figure 2 Roundness measurement by an angle probe: (a) without spindle error; (b) with spindle error

The differential output $m_{2D1A}(\theta)$ of the 2D1A mixed method can be denoted as

$$\begin{aligned} m_{2D1A}(\theta) &= m_A(\theta)(\tan\alpha + \cot\beta) \\ &\quad - m_C(\theta)/\sin\beta + R_r\mu_B(\theta)/\cos\alpha \\ &= r(\theta)(\tan\alpha + \cot\beta) \\ &\quad - r(\theta+\beta)/\sin\beta \\ &\quad + R_r r'(\theta+\alpha)/\cos\alpha \end{aligned} \tag{6}$$

Consequently, the effect of the spindle error is eliminated.

The characteristics of the mixed method can be estimated by its transfer function,[21,22] which defines the relationship between the roundness error $r(\theta)$ and the differential output. Let the Fourier transforms of $r(\theta)$ and $m_{2D1A}(\theta)$ be $R(n)$ and $M_{2D1A}(n)$, respectively, the transfer function of the 2D1A mixed method can be defined by

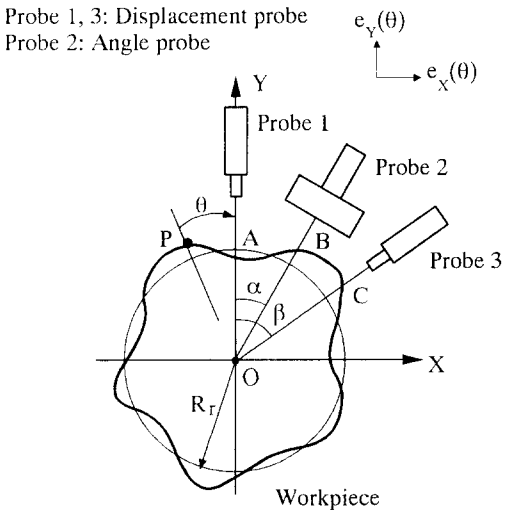

Figure 3 Roundness measurement by the 2D1A mixed method

$$\begin{aligned} H_{2D1A}(n) &= M_{2D1A}(n)/R(n) \\ &= \tan\alpha + \cot\beta - e^{jn\beta}/\sin\beta \\ &\quad + jne^{jn\alpha}/\cos\alpha \end{aligned} \tag{7}$$

where n is the frequency (the number of undulations per revolution). The transfer function $H_{m2D1A}(n)$ represents the complex harmonic sensitivity of the 2D1A mixed method. The amplitude (harmonic sensitivity) and the phase angle of $H_{m2D1A}(n)$ are expressed as follows.

$$\begin{aligned} |H_{2D1A}(n)| = \frac{1}{\cos\alpha\sin\beta}[&(\sin\alpha\sin\beta \\ &+ \cos\alpha\cos\beta - \cos\alpha\cos n\beta \\ &- n\sin n\alpha\sin\beta)^2 \\ &+ (n\cos n\alpha\sin\beta \\ &- \cos\alpha\sin n\beta)^2]^{1/2} \end{aligned} \tag{8}$$

$$\begin{aligned} \arg[H_{2D1A}(n)] = \tan^{-1}[&(n\cos n\alpha\sin\beta \\ &- \cos\alpha\sin n\beta)/(\sin\alpha\sin\beta \\ &+ \cos\alpha\cos\beta - \cos\alpha\cos n\beta \\ &- n\sin n\alpha\sin\beta)] \end{aligned} \tag{9}$$

We can also use one displacement probe and two angle probes to construct the mixed method. The probe outputs of the one displacement-two angle (1D2A) mixed method shown in *Figure 4* can be expressed as follows.

$$\mu_A(\theta) = r'(\theta) + e_X(\theta)/R_r \tag{10}$$

$$m_B(\theta) = r(\theta+\alpha) + e_X(\theta)\sin\alpha + e_Y(\theta)\cos\alpha \tag{11}$$

$$\begin{aligned} \mu_C(\theta) = r'(\theta+\beta) \\ + [e_X(\theta)\cos\beta - e_Y(\theta)\sin\beta]/R_r \end{aligned} \tag{12}$$

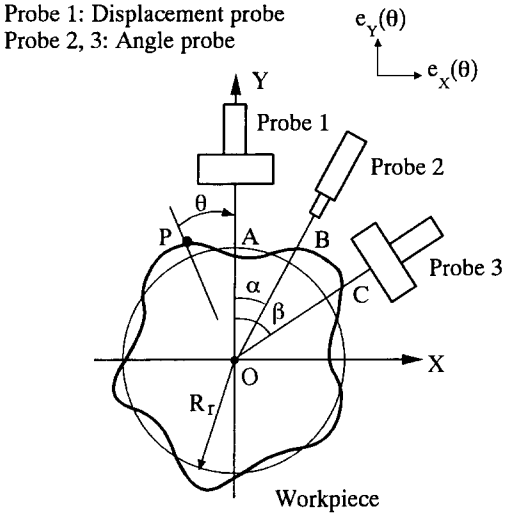

Figure 4 Roundness measurement by the 1D2A mixed method

The differential output in which the effect of the spindle error is canceled can be given by

$$\begin{aligned} m_{1D2A}(\theta) &= R_r\mu_A(\theta)(\tan\alpha + \cot\beta) \\ &\quad - m_B(\theta)/\cos\alpha - R_r\mu_C(\theta)/\sin\beta \\ &= R_r(\tan\alpha + \cot\beta)r'(\theta) \\ &\quad - r(\theta+\alpha)/\cos\alpha - R_r r'(\theta \\ &\quad + \beta)/\sin\beta \end{aligned} \tag{13}$$

The transfer function of the 1D2A mixed method can be defined as follows:

$$\begin{aligned} H_{1D2A}(n) &= M_{1D2A}(n)/R(n) \\ &= jn(\tan\alpha + \cot\beta) - e^{jn\alpha}/\cos\alpha \\ &\quad - jne^{jn\beta}/\sin\beta \end{aligned} \tag{14}$$

$$\begin{aligned} |H_{1D2A}(n)| = \frac{1}{\cos\alpha\sin\beta}[&(n\cos\alpha\sin n\beta \\ &- \cos n\alpha\sin\beta)^2 + (n\sin\alpha\sin\beta \\ &+ n\cos\alpha\cos\beta - \sin n\alpha\sin\beta \\ &- n\cos\alpha\cos n\beta)^2]^{1/2} \end{aligned} \tag{15}$$

$$\begin{aligned} \arg[H_{1D2A}(n)] = \tan^{-1}[&(n\sin\alpha\sin\beta + n\cos\alpha\cos\beta \\ &- \sin n\alpha\sin\beta \\ &- n\cos\alpha\cos n\beta)/(n\cos\alpha\sin\beta \\ &- \cos n\alpha\sin\beta)] \end{aligned} \tag{16}$$

With the angular distances α and β acting as parameters, the amplitudes of the transfer functions (harmonic sensitivities) of the two methods are plotted in *Figures 5* and *6*, respectively. As can be seen from the two figures, there is no frequency at which the harmonic sensitivity approaches zero, indicating that the mixed method can measure high-

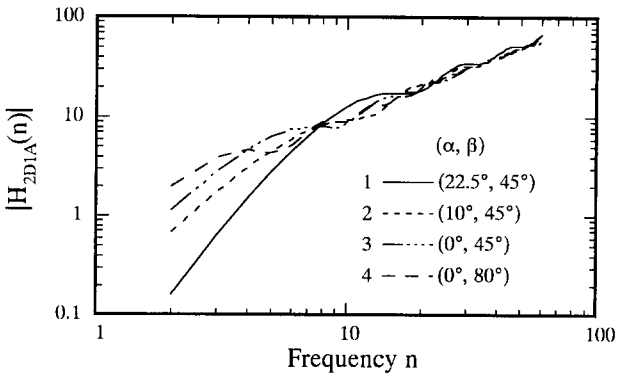

Figure 5 Transfer function of the 2D1A mixed method

frequency components correctly. In comparison with the 2D1A mixed method, the 1D2A mixed method is more sensitive when $n \leqslant 7$. On the other hand, the 2D1A mixed method is superior to the 1D2A mixed method in the higher-frequency range. The harmonic sensitivity of the 2D1A mixed method in low-frequency range and that of 1D2A mixed method in high-frequency range can be seen to be closely related to probe arrangement. As shown in *Figure 5*, the minimum harmonic sensitivity $|H_{2D1A}(2)|$ is only 0.16 for the symmetrical probe arrangement [$(\alpha, \beta) = (22.5°, 45°)$]. This value can be increased by changing the probe arrangement to one that is asymmetrical. For a fixed β, the largest $|H_{2D1A}(2)|$ is obtained when α is equal to 0° or β. In this probe arrangement, the angle probe and one of the displacement probes are placed at the same position. $|H_{2D1A}(2)|$ also improves as β increases. When $(\alpha, \beta) = (0°, 90°)$ or $(\alpha, \beta) = (90°, 90°)$, $|H_{2D1A}(2)|$ reaches its limiting value. In this probe arrangement, the 2D1A mixed method yields the most well-balanced harmonic response. The same can be said with regard to the 1D2A mixed method. We call the mixed method with this probe arrangement the orthogonal mixed method.

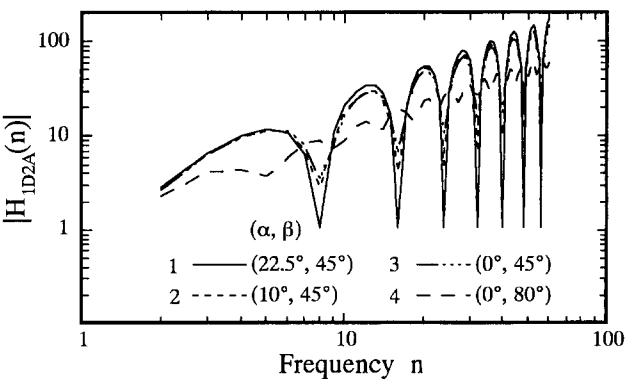

Figure 6 Transfer function of the 1D2A mixed method

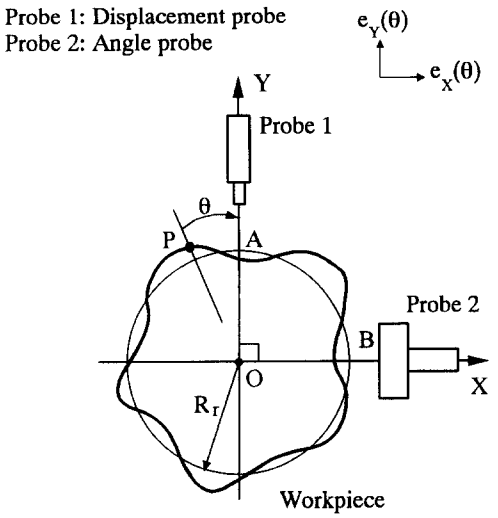

Figure 7 Roundness measurement by the orthogonal mixed method

The orthogonal mixed method

Figure 7 shows the principle of the orthogonal mixed method. The output $m_A(\theta)$ of the displacement probe and the output $\mu_B(\theta)$ of the angle probe can be expressed as follows:

$$m_A(\theta) = r(\theta) + e_Y(\theta) \tag{17}$$

$$\mu_B(\theta) = r'(\theta + \pi/2) - e_Y(\theta)/R_r \tag{18}$$

Therefore, the differential output $m_{om}(\theta)$, in which the roundness error is separated from the spindle error, can be denoted as

$$\begin{aligned} m_{om}(\theta) &= m_A(\theta) + R_r\mu_B(\theta) \\ &= r(\theta) + R_r r'(\theta + \pi/2) \end{aligned} \tag{19}$$

The transfer function $H_{om}(n)$ of the orthogonal mixed method can be defined as follows.

$$\begin{aligned} H_{om}(n) &= M_{om}(n)/R(n) \\ &= 1 + jne^{jn\pi/2} \end{aligned} \tag{20}$$

$$\begin{aligned} |H_{om}(n)| = [&(1 - n\sin n\pi/2)^2 \\ &+ (n\cos n\pi/2)^2]^{1/2} \end{aligned} \tag{21}$$

$$\begin{aligned} \arg[H_{om}(n)] = \tan^{-1}[&(n\cos n\pi/2)/ \\ &(1 - n\sin n\pi/2)] \end{aligned} \tag{22}$$

As can be seen from *Figure 8*, $H_{om}(n)$ yields a good characteristics. The minimum harmonic sensitivity $|H_{om}(2)|$ is 2.24.

As shown in *Figure 9*, if a setting error $\Delta\phi$ in the angular distance between the two probes exists, the differential output of the orthogonal mixed method becomes

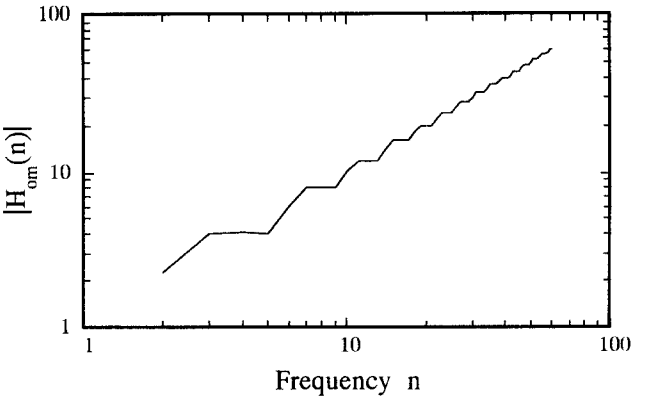

Figure 8 Transfer function of the orthogonal mixed method

$$\begin{aligned} m_e(\theta) &= r(\theta + \Delta\phi) + R_r r'(\theta + \pi/2) \\ &\approx r(\theta) + R_r r'(\theta + \pi/2) + \Delta\phi r'(\theta) \end{aligned} \tag{23}$$

An error $\Delta m_{om}(\theta)$ in the differential output can be seen to occur:

$$\Delta m_e(\theta) = \Delta\phi r'(\theta) \tag{24}$$

The evaluated Fourier transform $R_e(n)$ of the roundness error then becomes

$$\begin{aligned} R_e(n) &= M_e(n)/H_{om}(n) \\ &= R(n) + \Delta M_e(n)/H_{om}(n) \\ &= R(n) + \Delta R_e(n) \end{aligned}$$

where,

$$\Delta R_e(n) = \Delta M_e(n)/H_{om}(n) \tag{25}$$

Here, $R(n)$ is the real Fourier transform of the roundness error. $M_e(n)$ and $\Delta M_e(n)$ are the Fourier transforms of $m_e(\theta)$ and $\Delta m_e(\theta)$, respec-

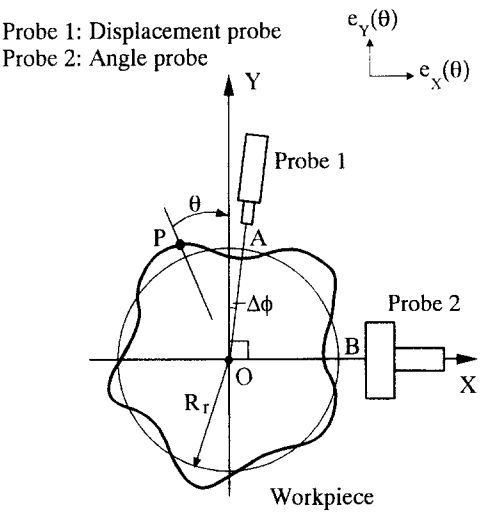

Figure 9 Setting error of angular distance

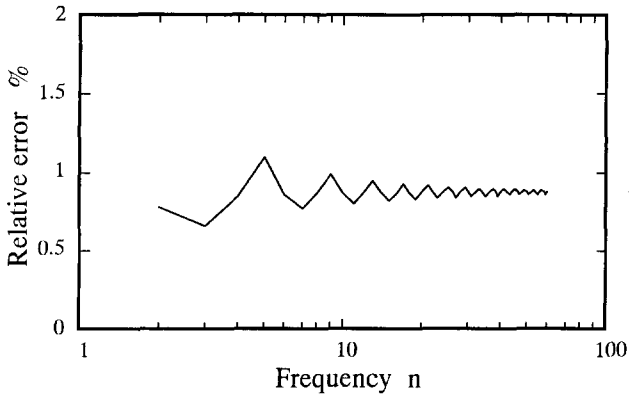

Figure 10 Error caused by the setting error of angular distance

tively. The relative error of $|R_e(n)|$ to $|R(n)|$ can then be evaluated as

$$\begin{aligned}\Delta E(n) &= 1 - |R_e(n)/R(n)| \\ &= |\Delta R_e(n)/R(n)| \\ &= n\Delta\phi/|H_{om}(n)| \end{aligned} \quad (26)$$

Figure 10 shows $\Delta E(n)$ plotted versus n when $\Delta\phi = 0.5°$. The largest error can be seen to occur at $n = 5(\Delta E(5) = 1.1\%)$.

Experiment

Principle of the optical sensor system

An optical sensor system consisting of one displacement probe and one angle probe with an angular distance of 90° was constructed to realize the orthogonal mixed method. Both the displacement probe and the angle probe use the principle of the critical angle method of total reflection.[23]

Figure 11 shows the optical schematic of the angle probe. The laser beam from a laser diode of 780-nm wavelength is collimated by a microlens and

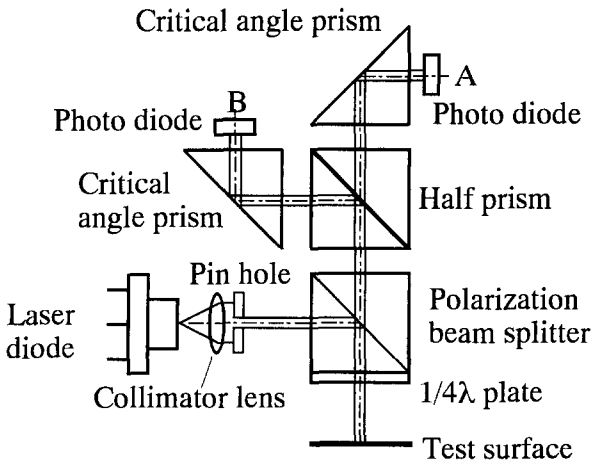

Figure 11 Optical schematic of the angle probe

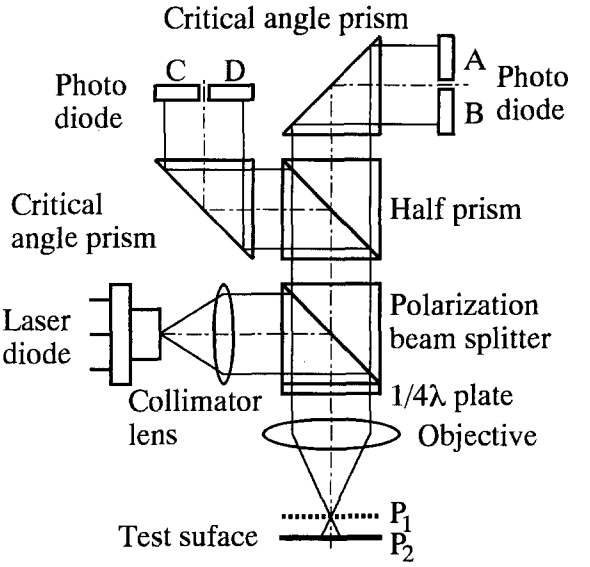

Figure 12 Optical schematic of the displacement probe

passes through a pinhole with a diameter of 0.1 mm. The beam is then bent by a polarization beam splitter and projected onto the test surface. The reflected beam from the test surface passing totally through the polarization beam splitter is split into two beams. After being reflected on the hypotenuse faces of the critical angle prisms, the beams finally reach photodiodes A and B. With respect to the incident beams, the hypotenuse faces are each arranged at an angle in the vicinity of the critical angle of air–glass boundary. When the test surface inclines, the output signals of the two photodiodes change in opposite ways: one increases, and the other decreases. The angular displacement $\Delta\theta$ of the test surface can be calculated from the output signals A and B of the photodiodes as follows.[24,25]

$$T_a(\Delta\theta) = (A - B)/(A + B) \quad (27)$$

where, $T_a(\Delta\theta)$ is defined as the output of the angle probe.

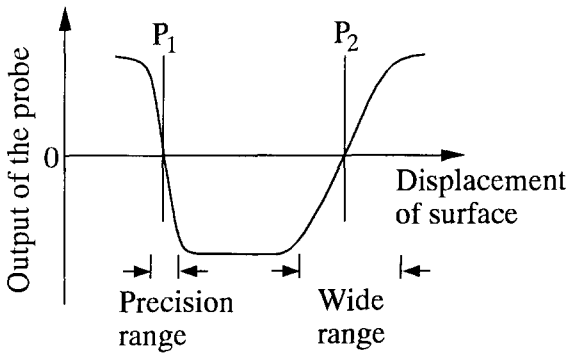

Figure 13 Precision range and wide range of the displacement probe

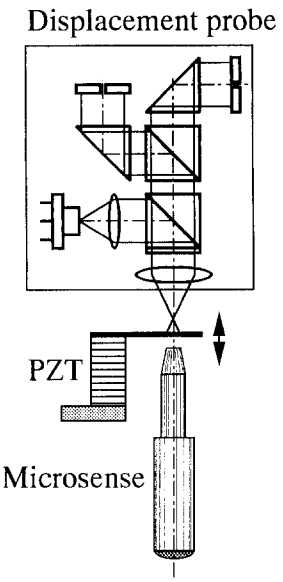

Figure 14 Experimental setup for displacement probe calibration

Figure 12 shows the optical schematic of the displacement probe.[26] The output $T_p(\Delta z)$ of the displacement probe can be expressed as follows.

$$T_p(\Delta z) = (A - B + C - D)/(A + B + C + D) \tag{28}$$

where Δz is the displacement of the test surface, and $A \sim D$ are the output signals of the photodiodes.

The relationship between $T_p(\Delta z)$ and Δz is shown in *Figure 13*. The area near P_1, which is the focal plane of the objective, is called the precision range. Another area, the wide range,[27,28] is also sensitive to the displacement. In the precision range, the light spot size is approximately 2 μm, and that in the wide range is approximately 0.1 mm. To match the light spot size of the displacement probe with that of the angle probe, the wide range was used. In addition, three-time-reflection-type critical-angle prisms[24] were used in the probes to improve the resolution.

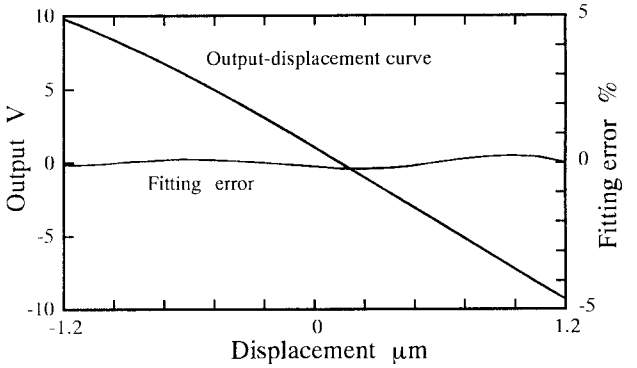

Figure 15 Calibrated results of the displacement probe

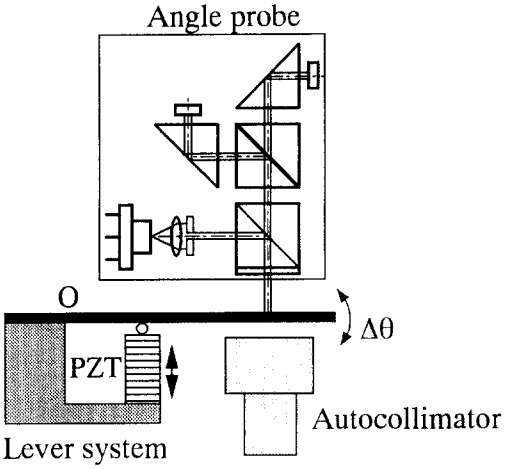

Figure 16 Experimental setup for angle probe calibration

Basic performance of the optical sensor system

Figure 14 shows the experimental setup for displacement probe calibration. A capacitance-type displacement sensor (ADE Microsense) was used as the reference. The surface was moved using a piezoelectric transducer (PZT) actuator, and the displacement of the surface was simultaneously measured by the developed displacement probe and the Microsense. *Figure 15* shows calibration results obtained in two separate measurements. The residual error from fitting with a third-order polynomial is also plotted in this figure and can be seen to be approximately 0.5% of the calibration range. Comparison of the two results shows good repeatability.

Figure 16 shows the experimental setup for angle probe calibration. A Nikon photoelectric autocollimator was used as the reference. A lever system was used to introduce angular displace-

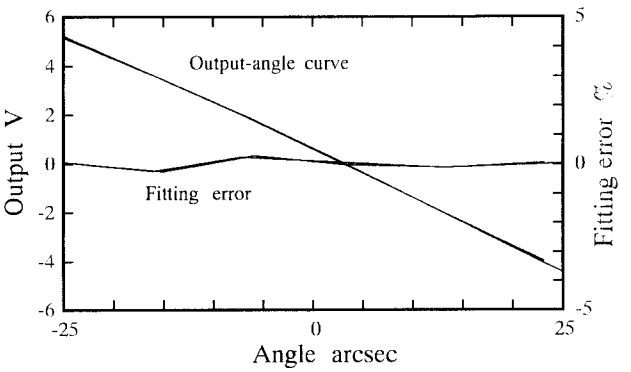

Figure 17 Calibrated results of the angle probe

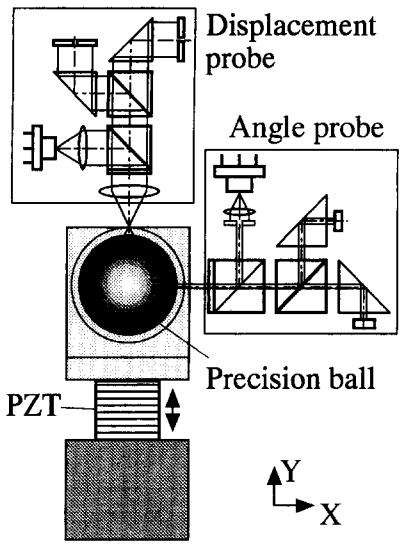

Figure 18 Experimental setup for investigating the characteristics of differential output

ment. The lever was driven using a PZT actuator so that the lever could rotate about its fulcrum. The angular displacement of the lever was measured simultaneously by the developed angle sensor and the autocollimator. Two separate calibration results are plotted in *Figure 17*. The residual error from fitting with a third-order polynomial is approximately 0.5% of the calibration range.

The experimental setup shown in *Figure 18* was used to investigate the feasibility of canceling the spindle error in the differential output of the orthogonal mixed method, which is defined in Equation (19). A precision ball with a diameter of 1 inch was used as the target. The displacement probe and the angle probe were set with an angular distance of 90°. The spindle error $e_Y(\theta)$ was introduced by moving the ball in the *Y*-direction by using a PZT. As shown in *Figure 19*, the spindle

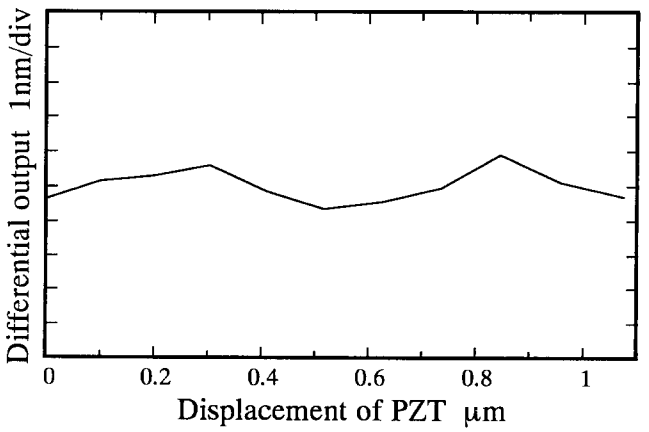

Figure 19 Differential output of the orthogonal mixed method

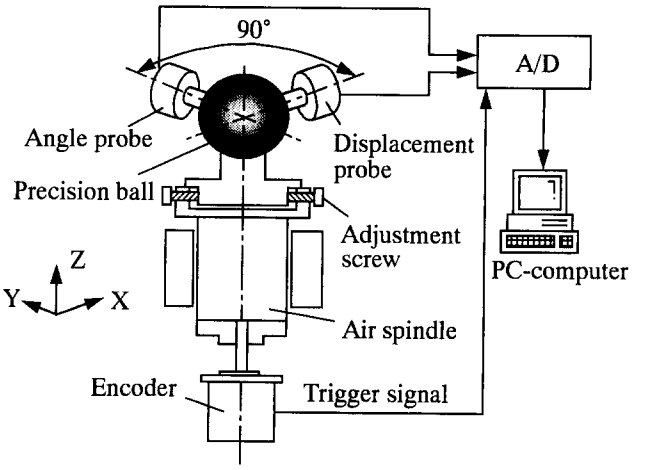

Figure 20 Experimental system for roundness measurement

error $e_Y(\theta)$ is canceled in the differential output of the orthogonal mixed method.

Roundness measurement

Figure 20 shows the experimental measurement system constructed for roundness measurement using the orthogonal mixed method. The measurement system consists of the developed displacement and angle probes, the precision ball shown in *Figure 18*, an air spindle, and an optical rotary encoder. The displacement probe and angle probe are set with an angular distance of 90°. The ball is mounted on the air spindle, and the profile of the ball can be sampled by the probes while the ball is rotating. The output signals of the probes are input to a personal computer via a 12-bit A/D converter. The rotational angle of the spindle was measured by the optical encoder. The positional signal of the optical encoder is sent to the A/D converter as a trigger signal. The output signals are sampled simultaneously in order to avoid errors attributable to the sampling time delay. The ball can be adjusted in the *X*- and

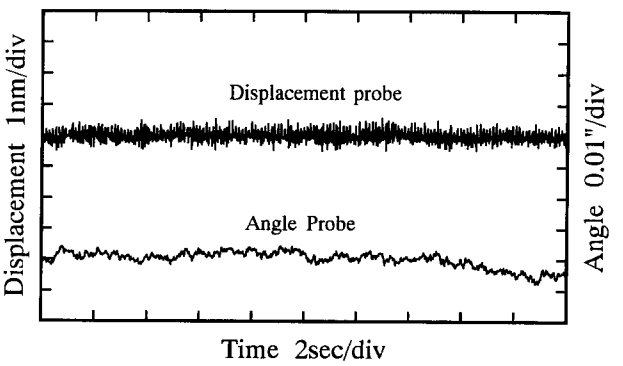

Figure 21 Stability of the probes

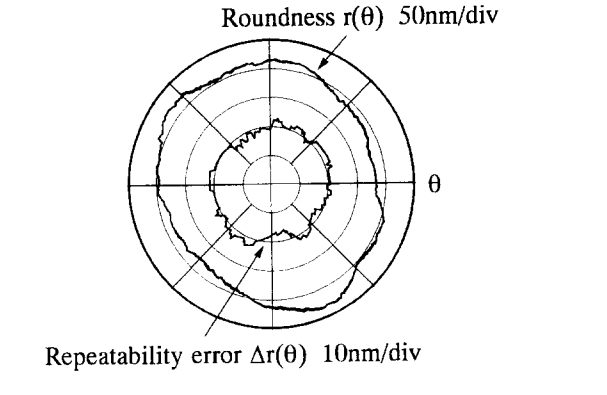

F(a) Polar plot of roundness error r(θ) and repeatability error Δr(θ)

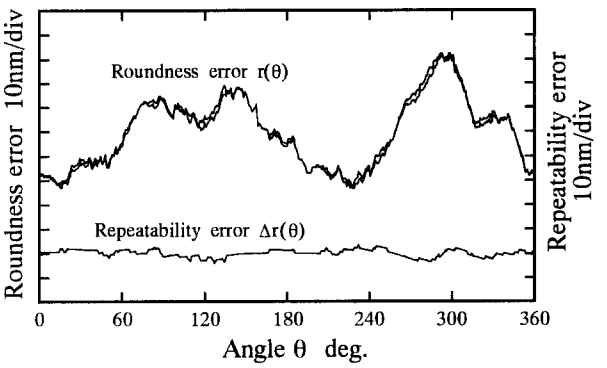

(b) Rectilinear plot of roundness error r(θ) and repeatability error Δr(θ)

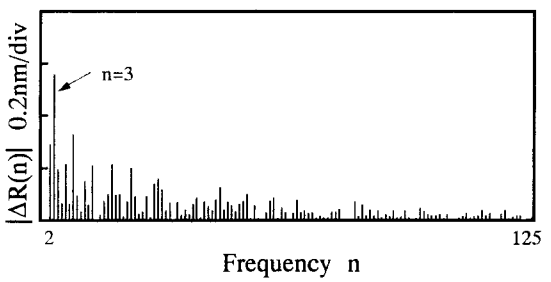

(c) Spectrum of the repeatability error

Figure 22 Measured roundness error: (a) polar plot of roundness error $r(\theta)$ and repeatability error $\Delta r(\theta)$; (b) rectilinear plot of roundness error $r(\theta)$ and repeatability error $\Delta r(\theta)$; (c) spectrum of the repeatability error

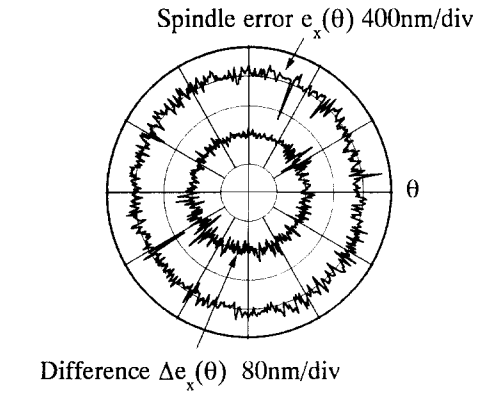

(a) Polar plot of spindle error $e_x(\theta)$ and difference $\Delta e_x(\theta)$

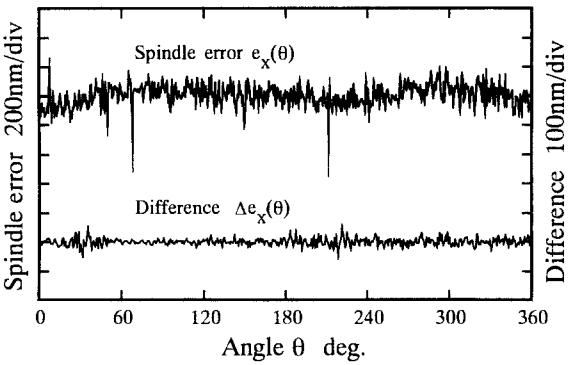

(b) Rectilinear plot of spindle error $e_x(\theta)$ and difference $\Delta e_x(\theta)$

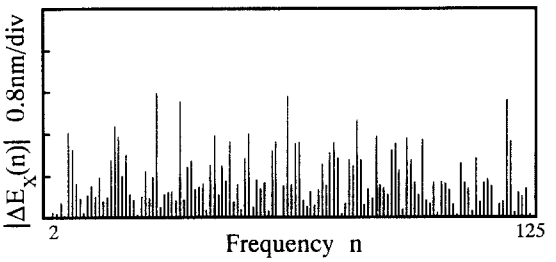

(c) Spectrum of the difference

Figure 23 Measured spindle error: (a) polar plot of spindle error $e_x(\theta)$ and difference $\Delta e_x(\theta)$; (b) rectilinear plot of spindle error $e_x(\theta)$ and difference $\Delta e_x(\theta)$; (c) spectrum of the difference

Y-directions by use of adjustment screws so that the eccentric error can be adjusted to fall within the measurement ranges of the probes. The probes are mounted on *XYZ* microstages, and the positions of the probes relative to the ball can be adjusted in the *X*-, *Y*-, and *Z*-directions.

Figure 21 shows the result of a stability test of the optical sensor. In the test, the output signals were sampled without rotating the ball. The displacement probe and the angle probe can be seen to have the stabilities of 1 nm and 0.01 in., respectively, in a test term of 20 s.

Figure 22 shows the measured roundness errors of two separate measurements and the repeatability error between the two measured results. The sampling number was 512. It can be seen that the roundness error is approximately 60 nm, and the repeatability error is approximately 5 nm. The largest repeatability error occurred at the third-order harmonic, and the value is approximately 0.6 nm. The repeatability error may be caused by the positioning error of sampling. The measured spindle errors of

the two repeated measurements and the difference between them are shown in *Figure 23*. The spindle error is approximately 800 nm, and the difference is approximately 140 nm. Vibration components are found in the spindle errors. Comparison of the results plotted in *Figures 22* and *23* shows that the roundness error is separated from large spindle errors with high repeatability, thus confirming the effectiveness of the orthogonal mixed method.

Conclusions

1. The effectiveness of the two displacement-one angle (2D1A) mixed method and that of the one displacement-two angle (1D2A) mixed method were discussed. Both of these methods can separate the roundness error from the spindle error with high accuracy. In the low-frequency range, the 1D2A mixed method is more sensitive than the 2D1A mixed method. In the high-frequency range, the 2D1A mixed method is superior to the 1D2A mixed method.
2. The characteristics of the 2D1A mixed method and the 1D2A mixed method were analyzed with regard to probe arrangement. It was verified that well-balanced harmonic response can be achieved over the entire frequency range when the angular distance between the angle probe, and the displacement probe is set to be 90°. The mixed method employing this probe arrangement is called the orthogonal mixed method. This probe arrangement is also the simplest one, because separation of the roundness error from the spindle error requires only one displacement probe and one angle probe.
3. An optical sensor system consisting of one displacement probe and one angle probe was constructed to realize the orthogonal mixed method. The displacement probe and the angle probe both use the critical angle method of total reflection, and they have stabilities of 1 nm and 0.01 in., respectively.
4. An experimental measurement system for roundness measurement based on the orthogonal mixed method was constructed. The effectiveness of the orthogonal mixed method was confirmed by the experimental results.

Acknowledgments

The authors thank S. Fukushima of Canon Ltd. and E. Gleason of Micro Surface Engr. Inc. for providing the air spindle and the precision ball, respectively. Financial support was provided by a grant-in-aid for scientific research of The Ministry of Education of Japan and the Mechatronics Scientific Foundation.

References

1 Whitehouse, D. J. "Some theoretical aspects of error separation techniques in surface metrology," *J Phys E: Sci Instrum*, 1976 **9**, 531–536
2 Ozono, S. "On a new method of roundness measurement based on the three points method," Proceedings of the International Conference on Production Engineering, Tokyo, 1974, 457–462
3 Kakino, Y. and Kitazawa, J. "In situ measurement of cylindricity," *Ann CIRP*, 1978, **27**, 371–375
4 Shinno, H., Mitui, K., Tatsue, Y., Tanaka, N. and Tabata, T. "A new method for evaluating error motion of ultra precision spindle," *Ann CIRP*, 1987, **36**, 381–384
5 Zhang, H., Yun, H. and Li, J. "An on-line measuring method of workpiece diameter based on the principle of three-sensor error separation," *Proc IEEE* 1990, **3**, 1308–1312
6 Fan, Y., Zhang, S. and Xu, W. "Kinematic and mathematical research on three-point method for in-process measurement and its applications in engineering," Proceedings of the 7th International Precision Engineering Seminar, Kobe, 1993, 318–328
7 Kato, H., Nakano, Y. and Nomura, Y. "Development of in-situ measuring system of circularity in precision cylindrical grinding," *Int J JSPE*, 1990, **24**, 130–135
8 Kato, H., Song, R. and Nomura, Y. "In-situ measuring system of circularity using an industrial robot and a piezoactuator," *Int J JSPE*, 1991, **25**, 130–135
9 Gleason, E. and Schwenke, H. "Spindleless instrument for the roundness measurement of precision balls," Proceedings of the ASPE 11th Annual Meeting, 1996, 167–171
10 Ozono, S. and Hamano, Y. "On a new method of roundness measurement based on the three-point method, 2nd report, Expanding the measurable maximum frequency," Proceedings of the annual meeting of JSPE, 1976, 503–504 (in Japanese)
11 Moore, D. "Design considerations in multiprobe roundness measurement," *J Phys E: Sci Instrum*, 1989, **9**, 339–343
12 Sonozaki, S. and Fujiwara, H. "Simultaneous measurement of cylindrical parts profile and rotating accuracy using multi-three-point-method," *Int J JSPE*, 1989, **23**, 286–291
13 Zhang, G. X. "Four-point method of roundness and spindle error measurements," *Ann CIRP*, 1993, **42**, 593–596
14 Kiyono, S. and Gao, W. "Estimation and improvement of accidental and systematic errors in profile measurement using software datum," *Trans JSME*, 1992, **58**, 2262–2267 (in Japanese)
15 Gao, W., Kiyono, S. and Nomura, T. "New multiprobe method of roundness measurements," *Prec Eng*, 1996, **19**, 37–45
16 Nunome, K., Tsukamoto, M., Yatagai, T. and Saito, H. "Interferometer for measuring the surface shape of a ball bearing raceway," *Appl Optics*, 1985, **24**, 3791–3796
17 Klingsporn, P. E. "Use of a laser interferometric displacement-measuring system for noncontact positioning of a sphere on a rotation axis through its center and for measuring the spherical contour," *Appl Optics*, 1985, **18**, 2881–2890
18 Ennos, A. E. and Virdee, M. S. "Precision measurement of surface form by laser autocollimation," *SPIE*, 1983, **398**, 252–257
19 Ennos, A. E., and Virdee, M. S. "High-accuracy profile measurement of quasi-conical mirror surfaces by laser autocolimation," *Prec Eng*, 1982, **4**, 5–8
20 Evan, J. D. "Method for approximating the radius of curvature of small concave spherical mirrors using a He–Ne laser," *Appl Optics*, 1971, **10**, 995–996
21 Hanmming, R. W. *Digital Filters*, New York: Prentice-Hall, 1977, Chs. 2, 3 (translated into Japanese by H. Miyagawa and H. Jideki, Kagaku-Gijyutu Publishing, 1980)
22 Kiyono, S. and Gao, W. "Profile measurement of machined surface with a new differential method," *Prec Eng*, 1994, **16**, 212–218

23 Jenkins, F. A. and White, H. E. *Fundamentals of Optics*, New York: McGraw-Hill, 1976, ch 2
24 Huang, P., Kiyono, S. and Kamada, O. "Angle measurement based on the internal-reflection effect: A new method," *Appl Optics*, 1992, **31,** 6047–6055
25 Huang, P. and Ni, J. "Angle measurement based on the internal-reflection effect and the use of the right-angle prisms," *Appl Optics*, 1995, **34,** 4976–4981
26 Kohno, T., Ozawa, N., Miyamoto, K. and Musha, T. "Highprecision optical surface sensor," *Appl Optics*, 1988, **27,** 103–108
27 Huang, P., Kiyono, S., Ohe, A., Kamada, O. and Satoh, E. "Smoothing characteristics of optical stylus," *Trans of JSME (C)*, 1991, **57,** 3710–3713 (in Japanese)
28 Kiyono, S., Yamatami, M. and Huang, P. "A new type of optical stylus with optical skid," *Proceedings of the ASPE 8th annual meeting*, 1983, 435–438